Complex dynamical behaviors of compact solitary waves in the perturbed mKdV equation*

Yin Jiu-Li(殷久利)†, Xing Qian-Qian(邢倩倩), and Tian Li-Xin(田立新)

Nonlinear Scientific Research Center, Faculty of Science, Jiangsu University, Zhenjiang 212013, *China*

(Received 12 December 2013; revised manuscript received 12 February 2014; published online 10 June 2014)

In this paper, we give a detailed discussion about the dynamical behaviors of compact solitary waves subjected to the periodic perturbation. By using the phase portrait theory, we find one of the nonsmooth solitary waves of the mKdV equation, namely, a compact solitary wave, to be a weak solution, which can be proved. It is shown that the compact solitary wave easily turns chaotic from the Melnikov theory. We focus on the sufficient conditions by keeping the system stable through selecting a suitable controller. Furthermore, we discuss the chaotic threshold for a perturbed system. Numerical simulations including chaotic thresholds, bifurcation diagrams, the maximum Lyapunov exponents, and phase portraits demonstrate that there exists a special frequency which has a great influence on our system; with the increase of the controller strength, chaos disappears in the perturbed system. But if the controller strength is sufficiently large, the solitary wave vibrates violently.

Keywords: Melnikov method, compacted solitary waves, control threshold

PACS: 02.30.Jr, 02.60.Lj **DOI:** 10.1088/1674-1056/23/8/080201

1. Introduction

The mKdV equation

$$u_t + au^2u_x + u_{xxx} = 0, \tag{1}$$

arises as a model which has been used to depict acoustic waves in certain anharmonic lattices[1] and Alfvén waves in a collisionless plasma.[2] It also appears in the model of Schottky barrier transmission lines and traffic congestion.[3,4] As is well known, the mKdV equation admits the smooth solitary waves, which have some good properties of the anti-interference and stable long-distance propagation.[5–10]

Recently, a class of nonsmooth solitary wave solutions, namely compacton solutions, was found from the mKdV equation.[11–13] They are compactly supported solitons with nonsmooth fronts. Quite a lot of research and studies have shifted towards compacton waves. More recently, normal compactons appear in nonlinear dispersive equations, such as nonlinear dispersive KdV equations[14] and nonlinear dispersive Schrödinger equations.[15] The more exciting aspect is that compacton waves have been found in the linear dispersive equation. Meanwhile, we should point out that the proof of the non-derivable compacton, which is a weak solution, has not been given. This article is concerned with all of these aspects. Further studies on different solitary wave solutions and their properties can be found in Refs. [16]–[30].

The purpose of this paper is to solve the following problems. Can the compacton wave be obtained from the phase portrait theory? How can the compacton be proved to be a weak solution? Can the compacton wave propagate stably as well as the chaos phenomenon, which may appear subjected to the external periodic perturbation? How can the chaos be well controlled?

As is well known, the majority of studies of chaos analysis and control target ordinary differential equations are subjected to the external perturbation. Less attention has been directed towards the chaotic behaviors of partial differential equations under different parameters of the periodic perturbed system, which is more suitable to practical models.[31–33]

Hence, we consider here equation (1) subjected to the periodic perturbation, i.e.,

$$u_t + au^2u_x + u_{xxx} = f(x,t), \tag{2}$$

where $f(x,t)$ is a periodic external perturbation.

Furthermore, we consider the following equation with a certain controller, which has the function of damping (see Ref. [15]) , i.e.,

$$u_t + au^2u_x + u_{xxx} = f(x,t) - \bar{k}(u)_{xx}. \tag{3}$$

The rest of the present paper is organized as follows. In Section 2, we analyze the bifurcation and phase portraits of the mKdV system. We use the Melnikov theorem to determine the threshold conditions for the occurrence of chaos and control of chaos in Section 3. In Section 4, numerical results for the nonlinear dispersive system under different parameters are given. Finally in Section 5, we draw some conclusions from the present study.

2. Phase portraits and weak-compacton solutions

Setting the traveling wave solution $u(x,t) = \varphi(\xi)$ and $f(x,t) = \bar{r}\sin w(x-ct)$, and using $\xi = x - ct$, equation (1) re-

*Project supported by the National Natural Science Foundation of China (Grant No. 11101191).

†Corresponding author. E-mail: yjl@ujs.edu.cn

© 2014 Chinese Physical Society and IOP Publishing Ltd

duces to the following form

$$-c\phi' + a\phi^2\phi' + \phi''' = \bar{r}\sin w\xi - \bar{k}\phi'', \tag{4}$$

where " $'$ " denotes the derivative with respect to ξ, c is the light speed in a vacuum, a is the parameter of the nonlinear dispersion term, $\bar{r}$ is the amplitude of the perturbation, and $a, c, \bar{r}$ are real constants and $\bar{r} = -w\varepsilon r$. Integrating Eq. (4) with respect to ξ, we obtain

$$-c\phi + \frac{a}{3}\phi^3 + \phi'' - l = \tilde{r}\cos w\xi - \bar{k}\phi'. \tag{5}$$

For convenience, we assume that $y = \phi'$, $\tilde{r} = \varepsilon r$, $\bar{k} = \varepsilon k$, and $l = 0$, then equation (5) is changed into the following form

$$\frac{\mathrm{d}\phi}{\mathrm{d}\xi} = y, \quad \frac{\mathrm{d}y}{\mathrm{d}\xi} = c\phi - \frac{a}{3}\phi^3 + \tilde{r}\cos w\xi - \bar{k}y. \tag{6}$$

When $\varepsilon = 0$, equation (6) becomes

$$\frac{\mathrm{d}\phi}{\mathrm{d}\xi} = y, \quad \frac{\mathrm{d}y}{\mathrm{d}\xi} = c\phi - \frac{a}{3}\phi^3. \tag{7}$$

Then, the system (6) is converted into an unperturbed system (7) with the following Hamiltonian function

$$H(\phi, y) = y^2 - c\phi^2 + \frac{a}{6}\phi^4 = h, \tag{8}$$

where h is a constant, and the potential function

$$V(\phi, y) = -c\phi^2 + \frac{a}{6}\phi^4. \tag{9}$$

Some specific equilibrium points are discussed in more detail below.

(i) There are three fixed points: $C_1(-\sqrt{3c/a}, 0)$ and $C_2(\sqrt{3c/a}, 0)$ which are two regular centers with two zero eigenvalues, and $S_0(0,0)$ that is a saddle point.

(ii) There are two homoclinic orbits

$$T^{\pm}_{\mathrm{hom}} = [\phi^{\pm}_{h1}(t), \phi^{\pm}_{h2}(t)]$$

that are connected with the saddle point $S_0(0,0)$.

However, through some special phase orbits, we discuss one solitary solution of Eq. (1) (see Ref. [20]). When $a > 0$ and $c > 0$, we can obtain

$$\begin{aligned} h_{30} &= H(0,0) = 0, \\ h_{31} &= H(-\sqrt{3c/a}, 0) = -3c^2/12a, \\ h_{32} &= H(\sqrt{3c/a}, 0) = -3c^2/12a. \end{aligned}$$

When $h = h_{30} = 0$, the curves determined by $H_1(U, V) = h$ correspond to a homoclinic orbit of Eq. (8) (see Fig. 1(a)). We have the following parametric compacton solution of Eq. (4):

$$u(x,t) = \begin{cases} \dfrac{4\lambda}{3}\sqrt{\dfrac{2}{a}}\dfrac{\cos^2\lambda(x - 4\lambda^2 t)}{\left(1 - \dfrac{2}{3}\cos^2\lambda(x - 4\lambda^2 t)\right)}, & |x - 4\lambda^2 t| \le \dfrac{\pi}{2\lambda}, \\ 0, & \text{otherwise.} \end{cases} \tag{10}$$

Obviously, it is the peculiar solitary wave solution called a compacton solution. The phase portrait of the compacton wave (10) is shown in Fig. 1(b). Obviously, the compacton wave has an n-derivable point. We will prove that it is a weak solution in the following section.

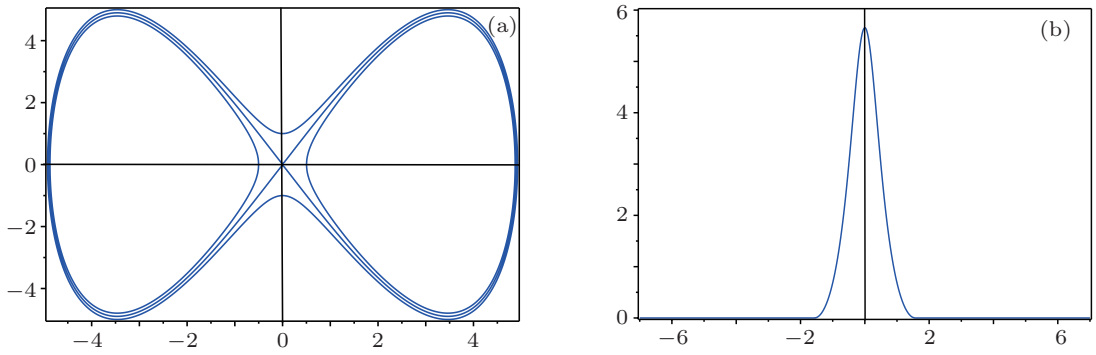


Fig. 1. (color online) (a) Phase portrait of system (7); (b) the profile of solitary solution.

Definition 1 The solitary wave solution $u \in L^1_{\mathrm{local}}(R^+, H^1_{\mathrm{local}}(R^1))$ is a weak solution to Eq. (1), if and only if $u \in L^1_{\mathrm{local}}(R^+, H^1_{\mathrm{local}}(R^1))$ and

$$\langle L, \varphi\rangle =: \int_0^{\infty}\int_{-\infty}^{+\infty}\left[u_t\varphi + \left(\frac{a}{3}u^3\right)_x\varphi + u_x\varphi_{xx}\right]\mathrm{d}x\mathrm{d}t = 0, \tag{11}$$

for any test function $\varphi(t,x) \in_0^{\infty} [R^+ \times R^1]$.

Proof Substituting u into the left-hand side of Eq. (11), we consider the compacton wave solution (10) for $|x - 4\lambda^2 t| \le \pi/2\lambda$ and $u = 0$ otherwise as well as $A = 4\sqrt{2}\lambda/3\sqrt{a}$. Then we obtain

$$\begin{aligned}\langle L,\varphi\rangle &= \int_0^{\infty} \mathrm{d}t \int_{-\pi/2\lambda+4\lambda^2 t}^{\pi/2\lambda+4\lambda^2 t} \left[u_t\varphi + \left(\frac{a}{3}u^3\right)_x \varphi + u_x\varphi_{xx}\right] \mathrm{d}x = \int_0^{\infty} \mathrm{d}t \int_{-\pi/2\lambda+4\lambda^2 t}^{\pi/2\lambda+4\lambda^2 t} \frac{36A\lambda^3\sin(2\lambda x-8\lambda^3 t)}{[\cos(2\lambda x-8\lambda^3 t)-2]^2}\varphi]\,\mathrm{d}x \\ &+ \int_0^{\infty} \mathrm{d}t \int_{-\pi/2\lambda+4\lambda^2 t}^{\pi/2\lambda+4\lambda^2 t} \left[\frac{-162aA\lambda^3\cos^5(\lambda x-4\lambda^3 t)\sin(\lambda x-4\lambda^3 t)}{[\cos(2\lambda x-8\lambda^3 t)-2]^4}\varphi\right]\mathrm{d}x \\ &+ \int_0^{\infty} \mathrm{d}t \int_{-\pi/2\lambda+4\lambda^2 t}^{\pi/2\lambda+4\lambda^2 t} \left[\frac{9A\lambda^3(-7\sin(2\lambda x-8\lambda^3 t)+16\sin(4\lambda x-16\lambda^3 t)+\sin(6\lambda x-24\lambda^3 t)}{[\cos(2\lambda x-8\lambda^3 t)-2]^4}\varphi\right]\mathrm{d}x \\ &= \cdots(\text{integration by parts}) \\ &= \int_0^{\infty} \mathrm{d}t \int_{-\pi/2\lambda+4\lambda^2 t}^{-\pi/2\lambda+4\lambda^2 t} \left[\frac{-18A\lambda(9aA^2-32\lambda^2)\cos^5(\lambda x-4\lambda^3 t)\sin(\lambda x-4\lambda^3 t)}{[\cos(2\lambda x-8\lambda^3 t)-2]^4}\right]\varphi\,\mathrm{d}x.\end{aligned}$$

Thus, if $A=4\sqrt{2}\lambda/3\sqrt{a}$, then $\langle L,\varphi\rangle=0$. This proves that solution (10) is a weak solution.

3. Chaos analysis for perturbed and controlled systems

Now we consider the chaotic threshold of one compacton solution of a system (12) subjected to one periodic perturbation. Undoubtedly, the homoclinic orbits will be broken in Eq. (6) and chaos is more likely to appear. When a proper controller is added to the perturbed system, the chaos phenomenon may be well controlled.

In this section, the chaotic behaviors of Eq. (6) will be discussed and $\varepsilon>0$ is a small parameter by the transformation $\tilde{r}\to\varepsilon r$ and $\bar{k}\to\varepsilon k$, hence equation (6) becomes

$$\frac{\mathrm{d}\phi}{\mathrm{d}\xi}=y,\quad \frac{\mathrm{d}y}{\mathrm{d}\xi}=c\phi-\frac{a}{3}\phi^3+\varepsilon r\cos w\xi-\varepsilon ky, \tag{12}$$

i) For $k=0$, the system (12) is a perturbed system. In our perturbed system (12), the Melnikov analysis would test the transverse intersection between stable and unstable manifolds, where the chaos may appear.

The derivative of solution (10) $u(x,t)$ with respect to $\tau=x-4\lambda^2 t$ is

$$\dot{u}(\tau)=\begin{cases}4\lambda\sqrt{\dfrac{2}{a}}\left(-\dfrac{4\lambda\cos^2\lambda\tau\sin\lambda\tau}{(3-2\cos^2\lambda\tau)^2}-\dfrac{2\lambda\cos\lambda\tau\sin\lambda\tau}{3-2\cos^2\lambda\tau}\right), & |\tau|\le\dfrac{\pi}{2\lambda},\\ 0, & \text{otherwise.}\end{cases} \tag{13}$$

Suppose that the unperturbed homoclinic orbits are written as

$$(u,\dot{u})=\left(\frac{4\lambda}{3}\sqrt{\frac{2}{a}}\frac{\cos^2\lambda\tau}{\left(1-\dfrac{2}{3}\cos^2\lambda\tau\right)},4\lambda\sqrt{\frac{2}{a}}\left(-\frac{4\lambda\cos^2\lambda\tau\sin\lambda\tau}{(3-2\cos^2\lambda\tau)^2}-\frac{2\lambda\cos\lambda\tau\sin\lambda\tau}{3-2\cos^2\lambda\tau}\right)\right),$$

for $|\tau|\le\pi/2\lambda$.

We note that $y_0(\tau)$ is a function of τ from $+\infty$ to $-\infty$ and suppose that $\tau=0$ and that $y_0(\tau)$ is an odd function for the homoclinic orbits, then the Melnikov function for system (12) can be given by

$$M(\tau_0)=\int_{-\infty}^{+\infty} y(\tau)[r\cos\omega(\tau+\tau_0)]\,\mathrm{d}\tau, \tag{14}$$

where τ_0 is the cross section of the Poincaré map and τ_0 may be interpreted as the initial value of the perturbation term.

We will compute $y(\tau)$ numerically in the next section using the obtained analytical expression of $y(\tau)b(\xi)$. The homoclinic orbits $\Gamma_{\mathrm{ho}}^{\pm}$ can be found by setting $H(u,\dot{u})=0$. Thus, the homoclinic orbits can be given as follows:

$$\begin{aligned}M(\tau_0) &= \int_{-\infty}^{+\infty} y(\tau)[r\cos\omega(\tau+\tau_0)]\,\mathrm{d}\tau \\ &= -2k\int_0^{\infty} y^2 d\tau - 2r\sin w\tau_0\int_0^{\infty} y\sin w\tau\,\mathrm{d}\tau \\ &= -2kB-2r\sin w\tau_0 A.\end{aligned}$$

Using the above results and Melnikov's theorem,[7,8] chaos may appear, if $M(\tau_0)=0$ and $M'(\tau_0)\neq 0$ for some values of ω and a set of parameters. If $M(\tau_0)$ has a simple zero and the corresponding critical parameter value is

$$\left(\frac{k}{r}\right)_0=\left|\frac{A}{B}\right|, \tag{15}$$

chaos may appear for certain parametric values which satisfy the following inequality

$$\frac{k}{r}\le\left(\frac{k}{r}\right)_0. \tag{16}$$

ii) For $k>0$, system (12) is a controlled system. Based on the Melnikov theory, the proper parameter of the controller can be chosen. Thus, the Melnikov function for system (12) can be given by

$$M_1(\tau_0)=\int_{-\infty}^{\infty} y_0(\tau)[ky(\tau)+r\cos\omega(\tau+\tau_0)]\,\mathrm{d}\tau$$

$$= 2k\int_0^{\pi/2\lambda} y_0^2(\tau)\,\mathrm{d}\tau - 2r\sin(\omega\tau_0) \times \int_0^{\pi/2\lambda} y_0(\tau)\sin(\omega\tau)\,\mathrm{d}\tau = -kB - r\sin w\tau_0 A. \quad (17)$$

Thus, if

$$|k| \le \left|\frac{rA}{B}\right|, \quad (18)$$

where

$$A = \int_{-\infty}^{\infty} \dot{u}(\tau)\sin w\tau\,\mathrm{d}\tau = \int_{-\pi/2}^{\pi/2} 4\lambda\sqrt{\frac{2}{a}}\left(-\frac{4\lambda\cos^2\lambda\tau\sin\lambda\tau}{(3-2\cos^2\lambda\tau)^2} - \frac{2\lambda\cos\lambda\tau\sin\lambda\tau}{3-2\cos^2\lambda\tau}\right)\sin w\tau\,\mathrm{d}\tau,$$

$$B = \int_{-\infty}^{+\infty}[\dot{u}(\tau)]^2 = \int_{-\pi/2}^{\pi/2}\left[4\lambda\sqrt{\frac{2}{a}}\left(-\frac{4\lambda\cos^2\lambda\tau\sin\lambda\tau}{(3-2\cos^2\lambda\tau)^2} - \frac{2\lambda\cos\lambda\tau\sin\lambda\tau}{3-2\cos^2\lambda\tau}\right)\right]^2\mathrm{d}\tau,$$

k denotes the strength of controller for the system, and r is the amplitude of the external perturbation.

For the surface of the intersection between the perturbed and unperturbed separatrices, the system always presents chaos for a fixed parameter. It is not difficult to find that the chaos threshold is dependent on parameters w, a, λ, and r/k.

According to the chaotic threshold in $(a, w, r/k)$ space and the chaotic threshold in $(\lambda, w, r/k)$ space, when the value of r/k is above the surface, chaos may appear. When the frequency taking timing system varies with a (or λ), the controller of system (15) should enhance the strength, with a (or λ) and w both increasing, the chaos of the system is reduced, and the system is easy to be controled.

(I) Chaos threshold of the peak of the solution in the (a, w, r/k) plane is shown in Fig. 2(a). The system subjected to the external periodic perturbation, can be controlled by the controller. When the frequency of the perturbation is fixed, the strength of the controller should be sufficiently large with the increase of the absolution of a. For the solitary wave speed, when w is very small, the chaos is difficult to control; inversely, if the value of w is large enough, chaos can be easily controlled.

(II) Chaos threshold of the peak of the solution in the (λ, w, r/k) plane is shown in Fig. 2(b). With the increase of the amplitude of the perturbation, the strength of the controller should be sufficiently large, with the speed of the solitary wave solution and the parameter of the convective term both fixed. However, the perturbed system can be controlled if the frequency is chosen to be sufficiently big or small. In short, there exists a maximum perturbed frequency. The system will be dramatically perturbed under this frequency.

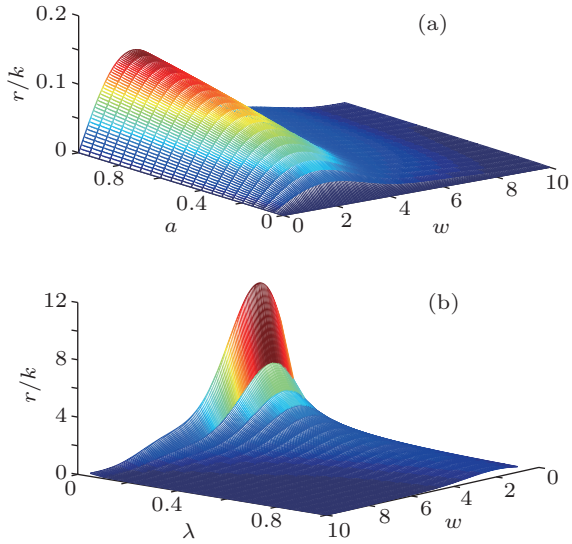


Fig. 2. (color online) (a) Chaotic threshold of system (12) in the (a, w, r/k) plane; (b) chaotic threshold in the (λ, w, r/k) plane.

4. Numerical simulation

The goal of the numerical simulation is to support the theoretical results of the previous section and to seek the controllable area. In this section, we will simulate the controllable regions of the system with different parameters. That is, we obtain the obvious relevance among these parameters.

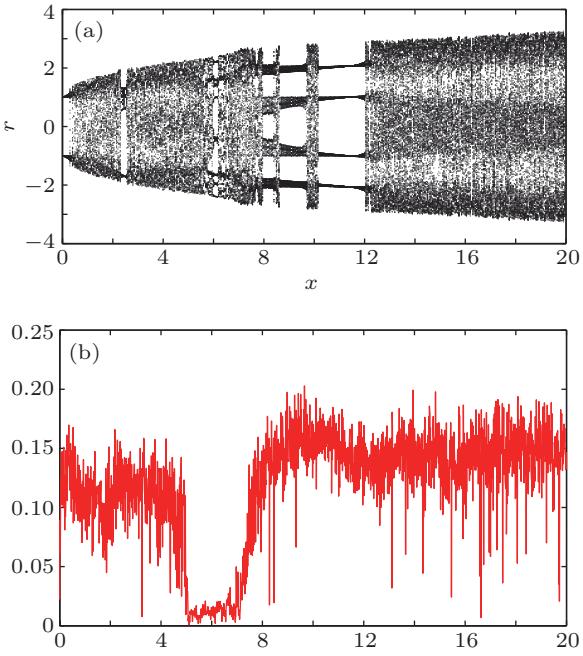


Fig. 3. (color online) (a) Bifurcation diagram of system (12) in the (r, x) plane; (b) maximum Lyapunov exponents corresponding to panel (a).

Numerical simulations are performed for the case of periodic perturbation of system (12). When the frequency of perturbation (15) w, the speed of system c, and the system parameter a are fixed, with varying the amplitude of the perturbation r, chaos will easily appear, which is shown in Figs. 3(a) and 3(b) where the maximum Lyapunov exponents are corresponding to Fig. 3(a). Time series plot and the phase diagrams

are shown in Fig. 5(a), chaos occurs in system (12). Meanwhile, when the amplitude of perturbation (15) r, the speed of system a, and the system parameter c are fixed, with varying the frequency of the perturbation w, the system will easily become chaotic, which is shown in Figs. 4(a) and 4(b) where the maximum Lyapunov exponents correspond to Fig. 4(a). The time series plot and the phase diagrams are shown in Fig. 5(b), chaos occurs in system (12).

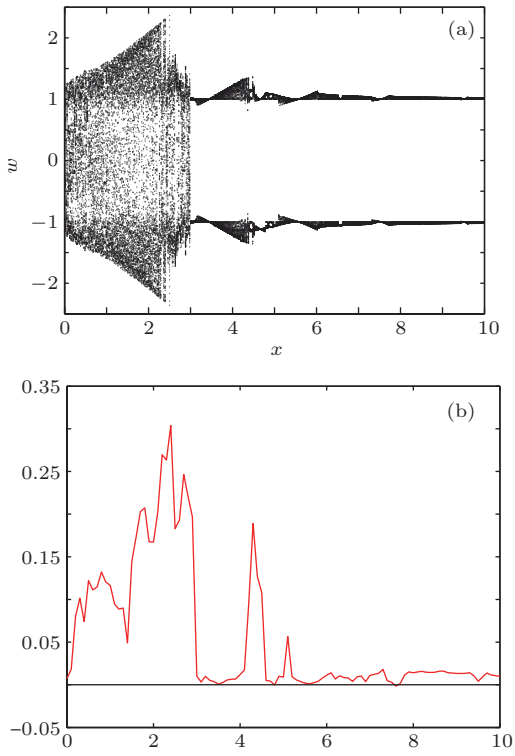


Fig. 4. (color online) (a) Bifurcation diagram of system (12) in the (w, x) plane; (b) maximum Lyapunov exponents corresponding to panel (a).

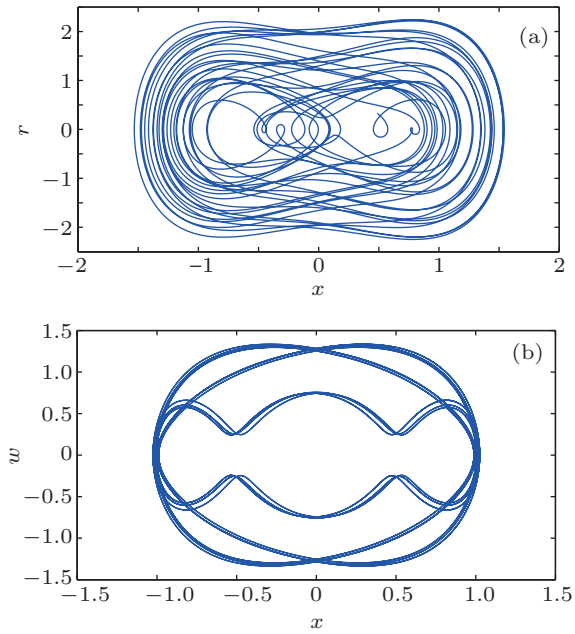


Fig. 5. (color online) (a) Phase diagram of system (12) in the (r, x) plane; (b) the phase diagram of system (12) in the (w, x) plane.

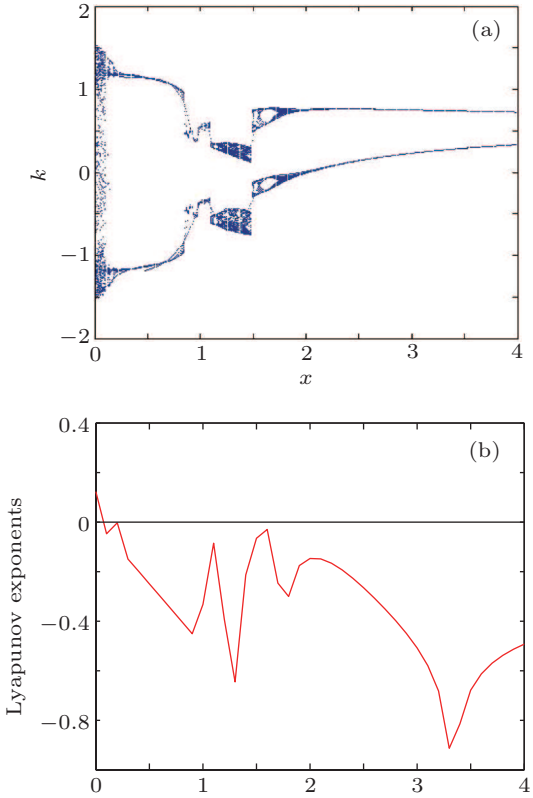


Fig. 6. (color online) (a) Bifurcation diagram of system (12) in the (k, x) plane; (b) maximum Lyapunov exponents corresponding to panel (a).

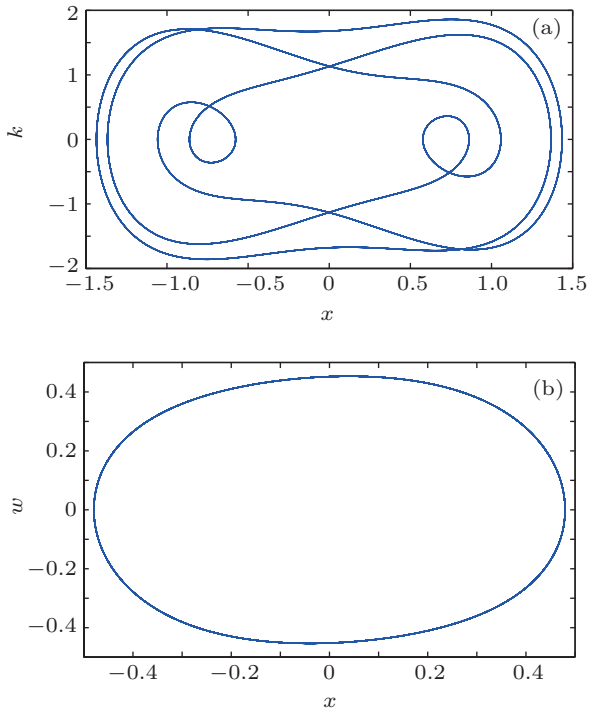


Fig. 7. (color online) (a) Phase diagram of system (12) in the (k,x) plane with $k = 0.1$; (b) phase diagram of system (13) in the (w, x) plane $k = 1.5$.

When the amplitude and frequency of perturbation (15) r and w, the speed of system a, and the system parameter c are fixed, with adding the controller ky, the system will be controlled, which is shown in Figs. 6(a) and 6(b) where the

maximum Lyapunov exponents correspond to Fig. 6(a). Time series plots under different controller strengths are shown in Fig. 7, and the chaos occurs in system (13).

5. Conclusions

In this paper, we analyzed the system under one frequency perturbation by using the Melnikov theory. When the system is disturbed by one-frequency perturbation, we use the controller to suppress the chaos. We further discuss the solitary solution of the stability of the system through varying the amplitude and the frequency of the perturbed system. In addition, we also present the chaotic threshold of the controlled system. It is shown that there is a special frequency which has a great influence on our system. With increasing the controller strength, the perturbed system will be in the stable state. But the solitary wave will vibrate violently when the controller strength is sufficiently large.

References

[1] Gaididei Y, Flytzanis N and Mertens F G 1995 *Physica D: Nonlinear Phenomenon* **82** 229
[2] Luo Q H and Melrose D 2007 *Planetary & Space Science* **55** 2281
[3] Ziegler V, Dinkel J, Setzer C and Lonngren K E 2001 *Chaos, Solitons and Fractals* **12** 1719
[4] Peng G H 2013 *Commun. Nonlinear Appl. Math. Comput.* **18** 2801
[5] Salas A H 2010 *Appl. Math. Comput.* **216** 2792
[6] Anco S C, Mohiuddin M and Wolf T 2012 *Appl. Math. Comput.* **219** 679
[7] Angulo J, Lopes O and Neves A 2008 *Nonlinear Anal.* **69** 1870
[8] Song M, Hou X J and Cao J 2011 *Appl. Math. Comput.* **217** 5942
[9] Anco S C, Ngatat N T and Willoughby M 2011 *Physica D: Nonlinear Phonomenon* **240** 1378
[10] Guo S M, Mei L Q, Fang Y and Qiu Z Y 2012 *Phys. Lett. A* **376** 158
[11] Hu X R, Chen Y and Huang F 2010 *Chin. Phys. B* **19** 080203
[12] Inc M 2007 *Appl. Math. Comput.* **184** 631
[13] Seadawy A R 2011 *Appl. Math. Comput.* **62** 3741
[14] Yin J L and Tian L X 2010 *Nonlinear Anal.: Theory, Method and Application* **73** 465
[15] Dereli Y 2012 *Engineering Analysis with Boundary Elements* **36** 1416
[16] Biswas A and Song M 2013 *Commun. Nonlinear Sci. Numer. Simul.* **18** 1676
[17] Song M, Liu Z R, Zerrad E and Biswas A 2013 *Frontiers of Math. China* **8** 191
[18] Song M, Bouthina A, Zerrad E and Biswas A 2013 *Chaos* **23** 033115
[19] Biswas A, Song M and Essaid Z 2013 *Int. J. Nonlinear. Sci. Numer. Simul.* **14** 317
[20] Song M, Ahmed B and Biswas A 2013 *J. Appl. Math.* **2013** 972416
[21] Antonova M and Biswas A 2009 *Commun. Nonlinear Sci. Numer. Simul.* **14** 734
[22] Houria T, Zlatko J and Biswas A 2014 *Appl. Math. & Informat. Sci.* **8** 113
[23] Polina R, Bouthina A and Biswas A 2014 *Appl. Math. & Informat. Sci.* **8** 485
[24] Zhang Z Y, Liu Z H, Miao X J and Chen Y Z 2010 *Appl. Math. & Comput.* **216** 3064
[25] Abdul H K, Houria T and Biswas A 2013 *Appl. Math. & Informat. Sci.* **7** 877
[26] Zhang Z Y, Li Y X, Liu Z H and Miao X J 2011 *Commun. Nonliear Sci. Numer. Simul.* **16** 3097
[27] Zhang Z Y, Liu Z H, Miao X J and Chen Y Z 2011 *Phys. Lett. A* **375** 1275
[28] Miao X J and Zhang Z Y 2011 *Commun. Nonlinear Sci. Numer. Simul.* **16** 4259
[29] Zhang Z Y, Xia F L and Li X P 2013 *Pramana J. Physics* **80** 41
[30] Wang Y F, Lou S Y and Qian X M 2010 *Chin. Phys. B* **19** 050202
[31] Zhang Z Y, Gan X Y, Yu D M, Zhang Y H and Li X P 2012 *Commun. Theor. Phys.* **57** 764
[32] Wazwaz A M 2004 *Appl. Math. & Comput.* **147** 439
[33] Wang F Z, Chen Z Q, Wu W J and Yuan Z Z 2007 *Chin. Phys.* **16** 3238